Gala Wind
3/15/2011

Analysis of differences between Science Test 8A and 8B

In this document we illustrate the differences in results between science tests 8A and 8B. Science test(ST) 8A is the baseline test. Science test 8B shows changes due to spatial interpolation of surface temperature and also due to substitution of NCEP GDAS "TMP:2 m above gnd" field (T2M) instead of "TMP:sfc" field (TSFC) for surface temperature. We use the surface temperature to calculate emission due to surface present in the 3.7μm signal. This emission, along with other emission components, must be removed before retrieval of cloud optical thickness and cloud effective radius could be attempted. The cloud optical properties retrieval uses reflected solar signal only. The suggestion for use of T2M instead of TSFC came from UW-Madison team. They have established that model output has better quality for the T2M field, particularly when sun angle is low. The impact of this science change affects 3.7μm retrieval only. We show cloud optical thickness here only for illustrative purposes.

We have examined impacts of these changes in science test of one-month duration for April 2005, Terra and Aqua MODIS. Figure 1 shows global monthly maps of 3.7μm retrievals for ice clouds with figure 1a containing result from science test 8A Terra and Aqua, figure 1b from science test 8B and figure 1c is the difference map between the two. Figure 2 shows global monthly maps of 3.7μm retrievals for liquid water clouds with same panel breakdown. Aqua MODIS shows a similar pattern, however the differences in ice cloud retrievals are more pronounced for Terra over high-elevation desert regions such as Pakistan and US Southwest. There the surface-level inversion may be strong enough to persist all the way until Terra's overpass time. Overall the impact is much more pronounced for ice clouds than for liquid water clouds. Extended liquid water cloud fields, such as marine stratocumulus, however do tend to be generally thicker and so effects of changes in amount of surface emission would tend to be minimized. Ice clouds are frequently

present as extended fields of thin cirrus that would be quite sensitive to amount of emission from surface present.

Next we looked in detail at areas where significant gradients of surface temperature exist and so sensitivity to changes in surface temperature field may be expected.

We have selected a granule near the Galapagos Islands, where coastal upwelling creates a significant gradient of surface temperature. Figures 3 and 4 show this result for Terra MODIS 2005 day 091, 16:50UTC. Figure 3a shows the RGB composite of the granule, which is dominated by liquid water clouds. Figure 3b shows the original surface temperature field used in science test 8A. Figure 3c shows the surface temperature field used in science test 8B. Figure 4a shows the retrieved cloud optical thickness, figure 4b and 4c show the retrieved 3.7μm cloud effective radius from science test 8A and 8B respectively. Figure 4d is the difference image for retrieved 3.7μm effective radii: ST8B-ST8A. Figure 5 shows the retrieval result for Aqua MODIS over the same area from 2005 day 091, 19:40UTC with panels labeled same as in figure 4. Figure 6 shows histograms of optical thickness and 3.7μm cloud effective radius for the Galapagos Islands case taken in a lat/lon box (UL,LR: (4, -104), (-12, -88)) degrees. Overall the impact of switching to T2M for this case is not very significant. We see a slight increase in retrieved effective radius when the T2M temperature is higher than TSFC and a slight decrease when T2M is lower than TSFC. This behavior is as expected because lower temperature will give smaller amount of emission to be subtracted, the remaining solar signal will increase and retrieved effective radius will then decrease. The impact on the mean retrieval is very small, as can be seen from Table 1. The histograms in Figure 6 show the localized per-bin impact.

Another case that we analysed is over western United States, where a frontal system creates a gradient in surface temperature over land. Figure 7 shows the RGB image and surface temperature fields. Figure 8 shows the retrieval results and differences for Terra MODIS 2005 day 091 18:15UTC. Figure 9 shows retrieval results and differences for Aqua MODIS 2005 day 091 at 19:55 UTC. Figure 10 shows histograms for ice and liquid water phase retrievals of cloud optical thickness

and 3.7μm cloud effective radius taken in a lat/lon box (UL,LR: (52,-115), (40, -95)) degrees. In this case, completely over land, Terra shows a more significant impact than Aqua. This could be attributed to diurnal variability in difference between TSFC and T2M fields. At time of morning overpass a part of the nighttime surface inversion may still persist, but would be completely gone by the time Aqua would pass over the area.

Third case we looked at is primarily ice cloud, there is not a lot of cloud in the scene overall, but we have a field of thin cirrus crossing a land/water boundary in northern Arabian Sea. Due to orbital gaps Aqua had no view, so this analysis is for Terra only. Figure 11 shows the RGB image and surface temperature fields. Figure 12 shows retrieval results and differences for Terra MODIS 2005 day 109, 06:35 UTC. Figure 13 shows histograms of cloud optical thickness and effective radius taken for the full granule. There was no real need to create a lat/lon box because we only have one instrument view.

This granule has a lot of thin cirrus present and shows statistically much more significant impact of change in surface temperature data source. In this case the T2M field is significantly lower over land and somewhat higher over ocean. The T2M field is more uniform across land / sea boundary and so the differences between land and ocean in this case are quite significant. Overall the ice effective radius retrievals have decreased by over a micron and liquid water by a quarter of a micron.

The last case we examined also shows a great deal of ice cloud over the northern Arabian Sea. We have both Aqua and Terra views in this case, however the cloud field is not as good as in the previous case. Figures 14, 15, 16 and 17 show the analysis of this case and histograms taken in a lat/lon box (UL,LR: (32, 56), (16, 72)) degrees.

In this case the diurnal pattern is not very visible for ice clouds with ice clouds showing hardly any change in retrieval mean, but is more significant for liquid water clouds. It is possible that the cloud field has changed somewhat and so the retrieval pattern is not as visible. It is still pronounced for liquid water clouds in the scene. They show a greater impact for Terra than for Aqua.

In this document we outlined retrieval changes that resulted from substitution of T2M GDAS field instead of TSFC as source for surface temperature information used as basis for calculation of surface emission amount. We show global monthly statistics and an in-depth look at a few interesting cases.

Case / lat,lon (UL) – (LR)	Phase	8A		8B		8B-8A	
		τ_c	$r_{e(\mu m)}$	τ_c	$r_{e(\mu m)}$	τ_c	$r_{e(\mu m)}$
T 2005.091.1650 (-4, -104) - (-12, -88)	Ice	17.68	18.70	17.68	18.69	0	-0.01
	Liquid	5.36	12.68	5.36	12.63	0	-0.05
A 2005.091.1940 (-4, -104) - (-12, -88)	Ice	0.41	---	0.41	---	0	---
	Liquid	5.13	12.76	5.13	12.65	0	-0.11
T 2005.091.1815 (52,-115) – (40, -95)	Ice	5.26	22.85	5.26	22.65	0	-0.2
	Liquid	4.39	17.13	4.39	16.95	0	-0.18
A 2005.091.1955 (52,-115) – (40, -95)	Ice	5.76	20.72	5.76	20.67	0	-0.05
	Liquid	3.27	13.78	3.27	13.71	0	-0.07
T 2005.109.0635 no box	Ice	4.48	27.54	4.48	26.17	0	-1.37
	Liquid	4.873	13.87	4.873	13.60	0	-0.27
T 2005.111.0625 (32, 56) – (16, 72)	Ice	5.13	28.36	5.13	28.38	0	+0.02
	Liquid	3.03	15.12	3.03	14.67	0	-0.45
A 2005.111.0930	Ice	7.36	30.69	7.36	31.29	0	+0.6
	Liquid	4.59	13.67	4.59	13.3	0	-0.37

Table 1: Mean values of optical thickness and 3.7μm cloud effective radius for all cases analyzed within box areas indicated for each granule.

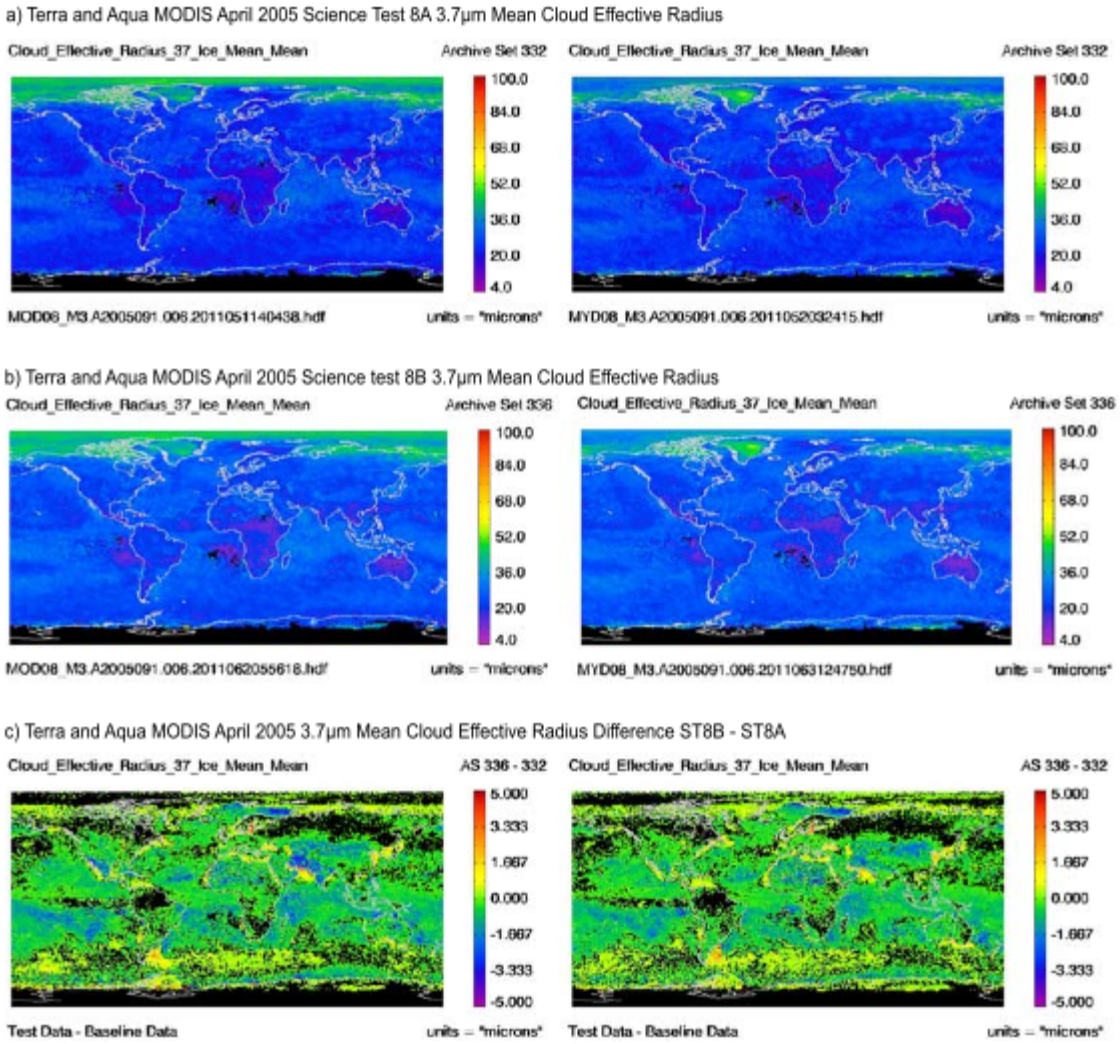

Figure 1: Monthly mean 3.7µm cloud effective radius retrievals for ice clouds from Terra and Aqua.

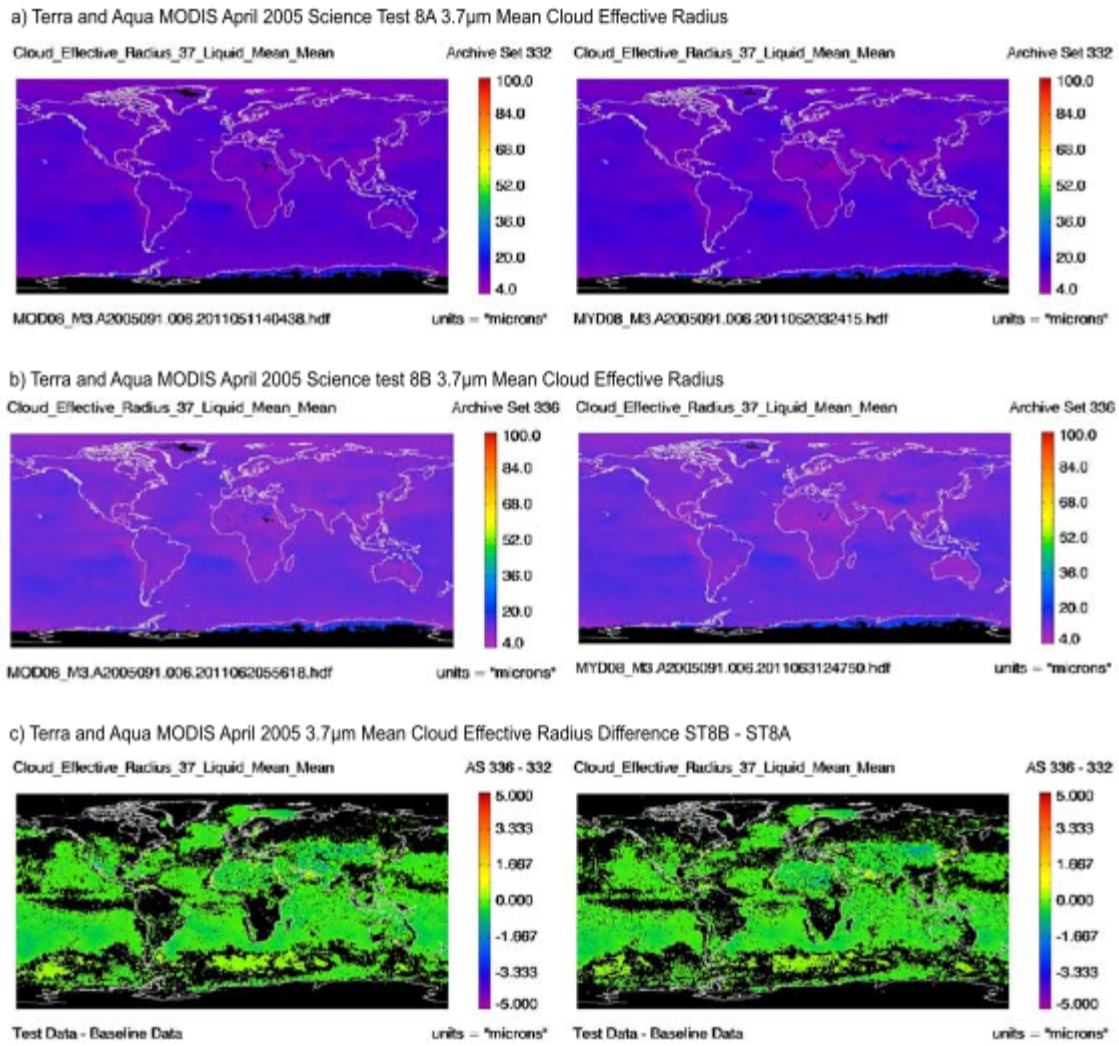

Figure 2: Monthly mean 3.7µm cloud effective radius retrievals for liquid water clouds from Terra and Aqua.

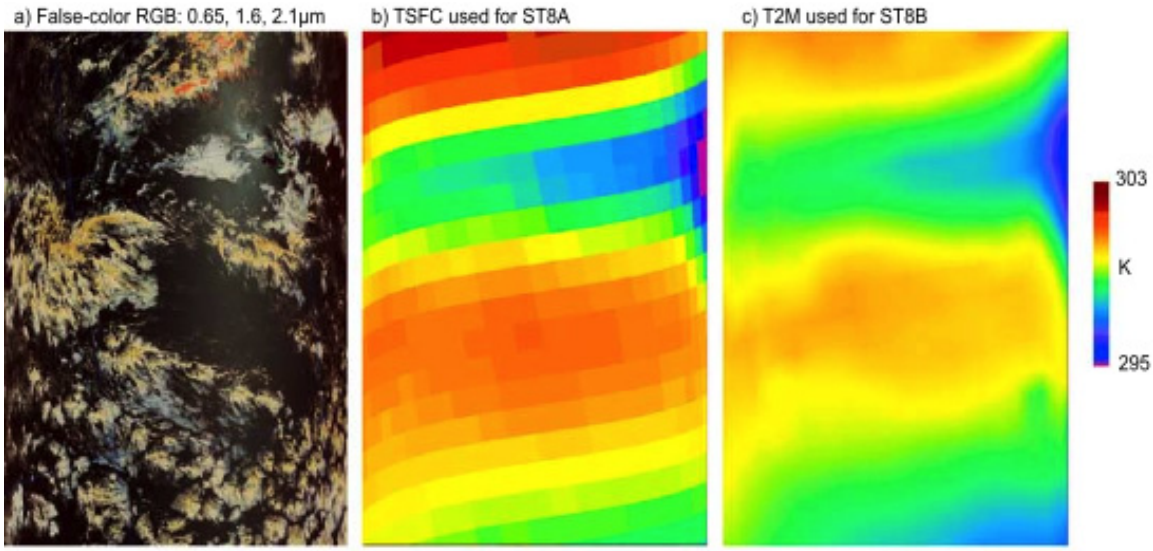

Figure 3: Terra MODIS 2005 day 091, 16:50 UTC. Panel a) shows the false-color RGB composite RGB: 0.65, 1.6, 2.1μm. Panel b) shows the original surface temperature field used in ST8A. Panel c) shows the new interpolated T2M-based surface temperature field.

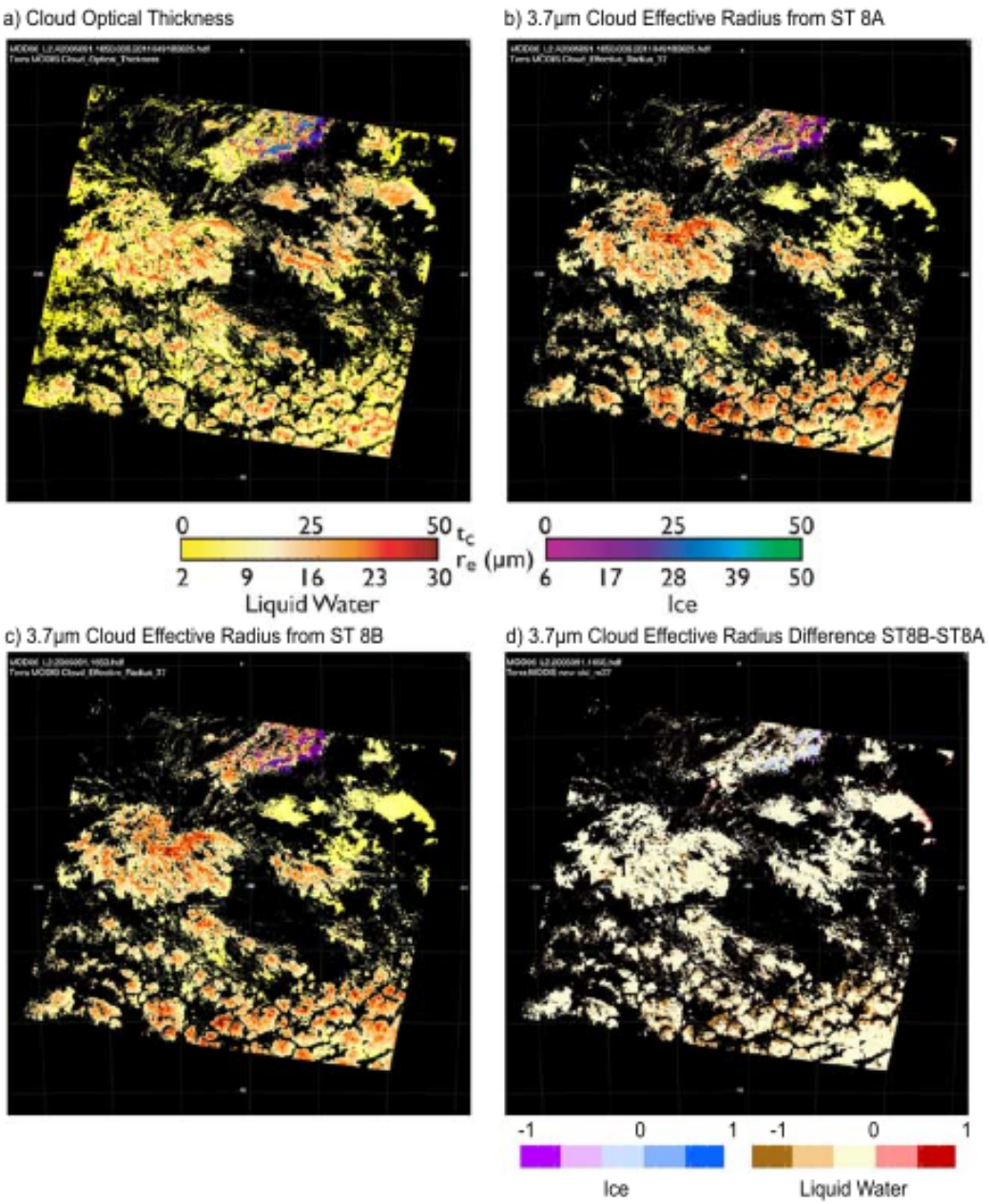

Figure 4: Terra MODIS 2005 day 091, 16:50 UTC, Eastern Pacific Ocean off Galapagos Islands. The panels illustrate the impact of changes between science test 8A and 8B as cloud optical thickness in panel a), 3.7µm cloud effective radius from ST8A in panel b), 3.7µm cloud effective radius from ST8B in panel c) and the difference image in panel d)

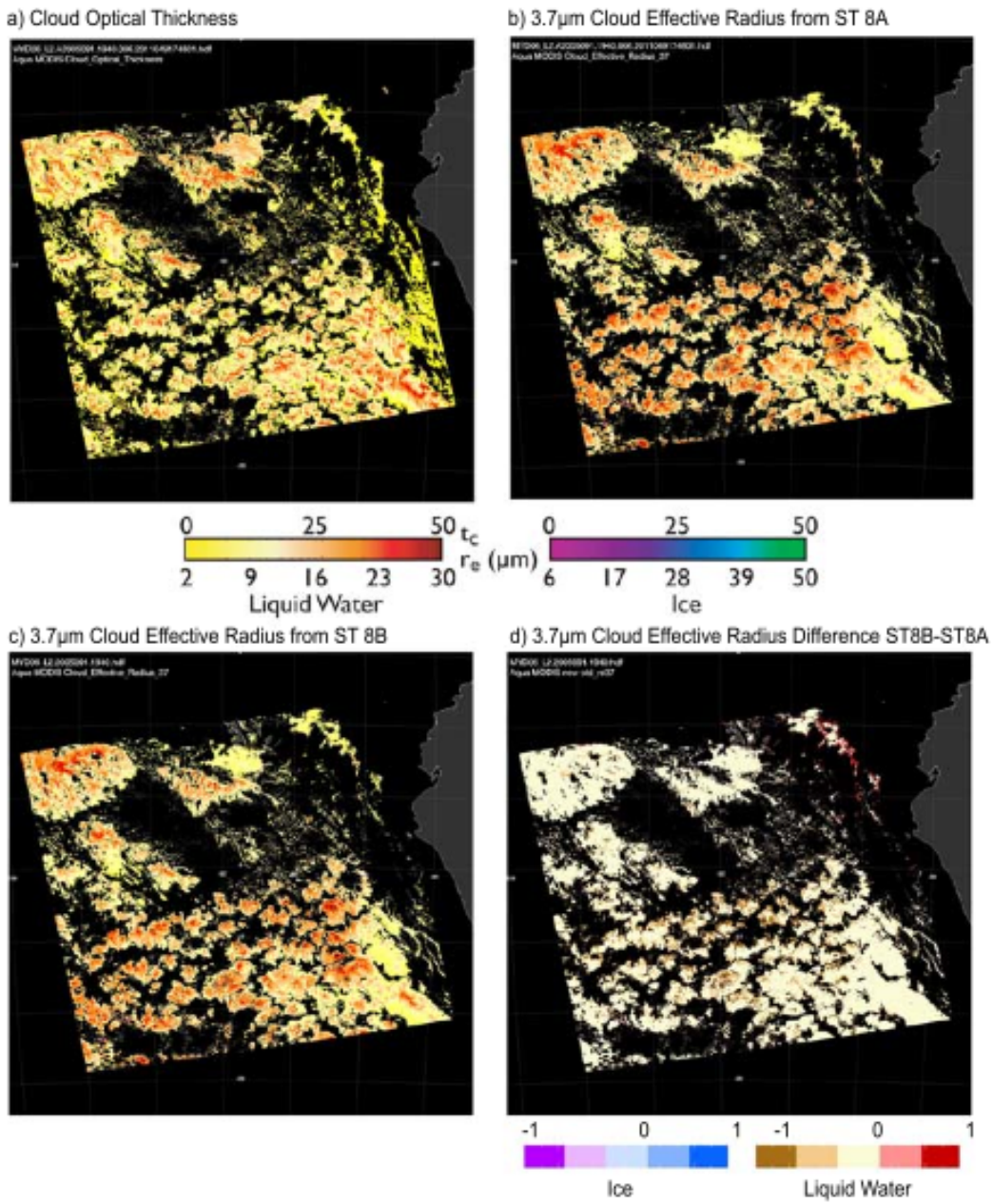

Figure 5: Aqua MODIS 2005 day 091, 19:40 UTC, Eastern Pacific Ocean off Galapagos Islands. The panels illustrate the impact of changes between science test 8A and 8B as cloud optical thickness in panel a), 3.7µm cloud effective radius from ST8A in panel b), 3.7µm cloud effective radius from ST8B in panel c) and the difference image in panel d)

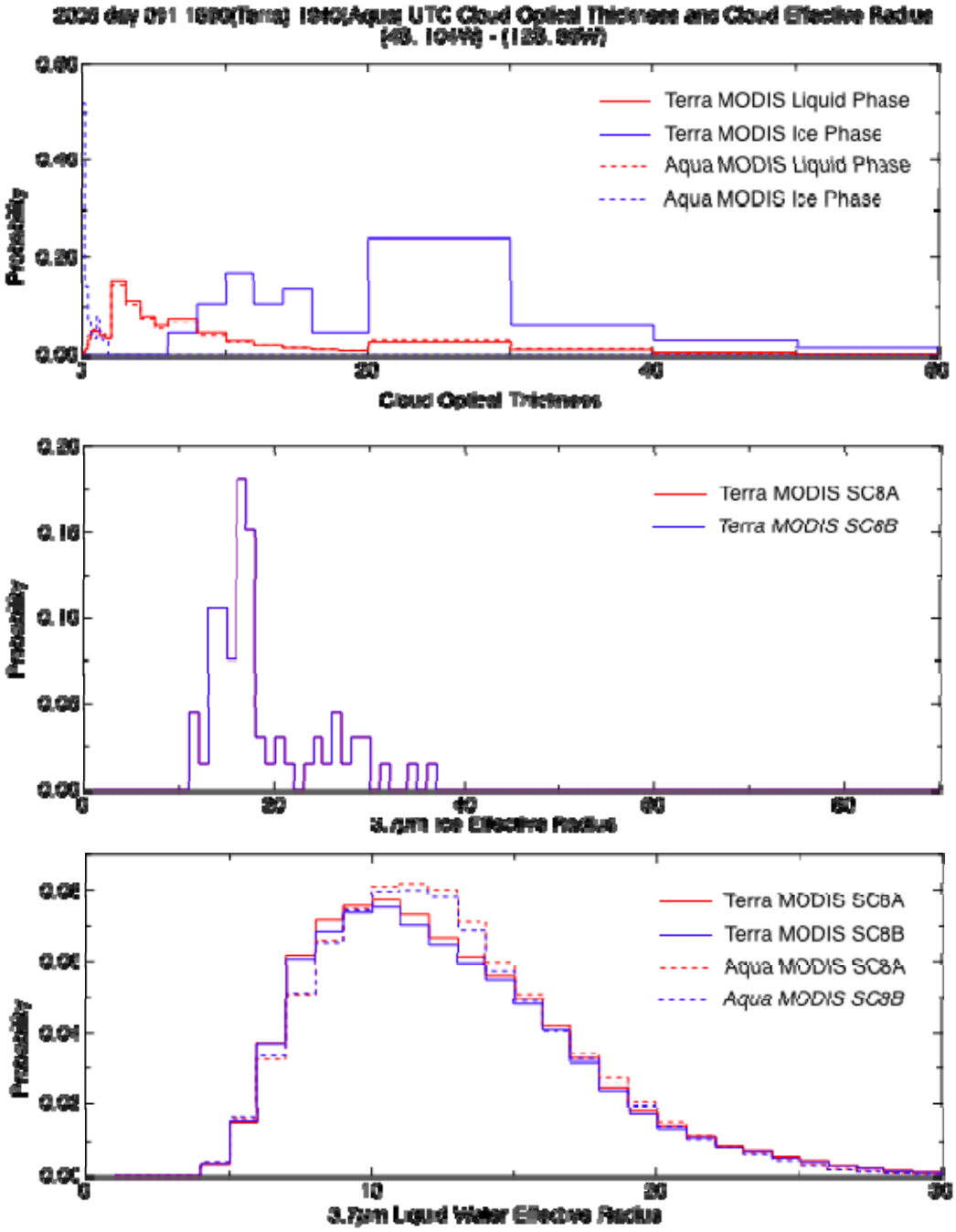

Figure 6: Histograms of retrieved optical thickness and 3.7μm cloud effective radius for the Galapagos case.

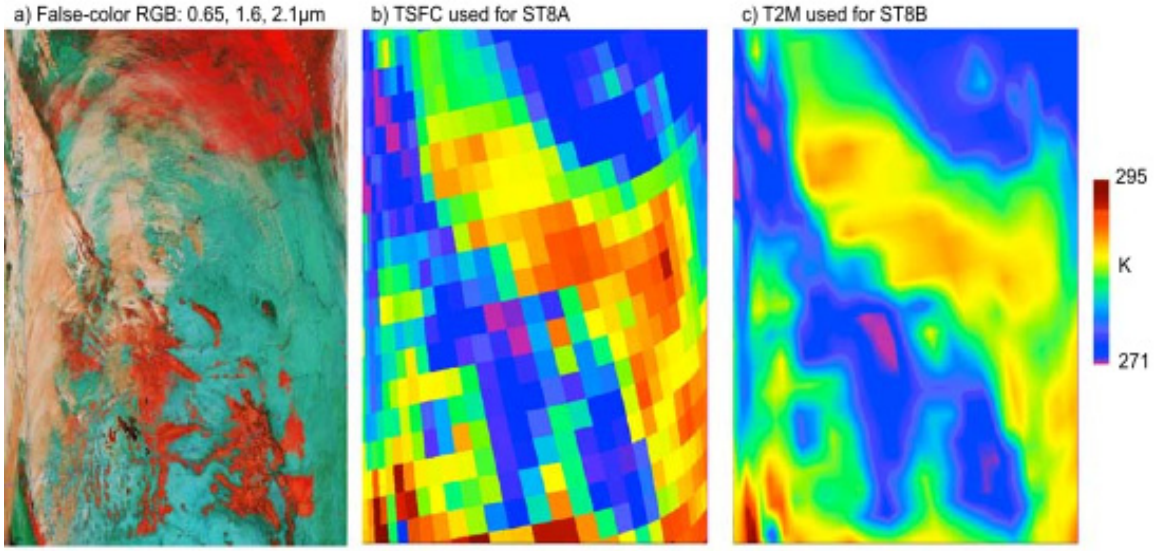

Figure 7: Terra MODIS 2005 day 091, 18:15 UTC. Panel a) shows the false-color RGB composite RGB: 0.65, 1.6, 2.1μm. Panel b) shows the original surface temperature field used in ST8A. Panel c) shows the new interpolated T2M-based surface temperature field.

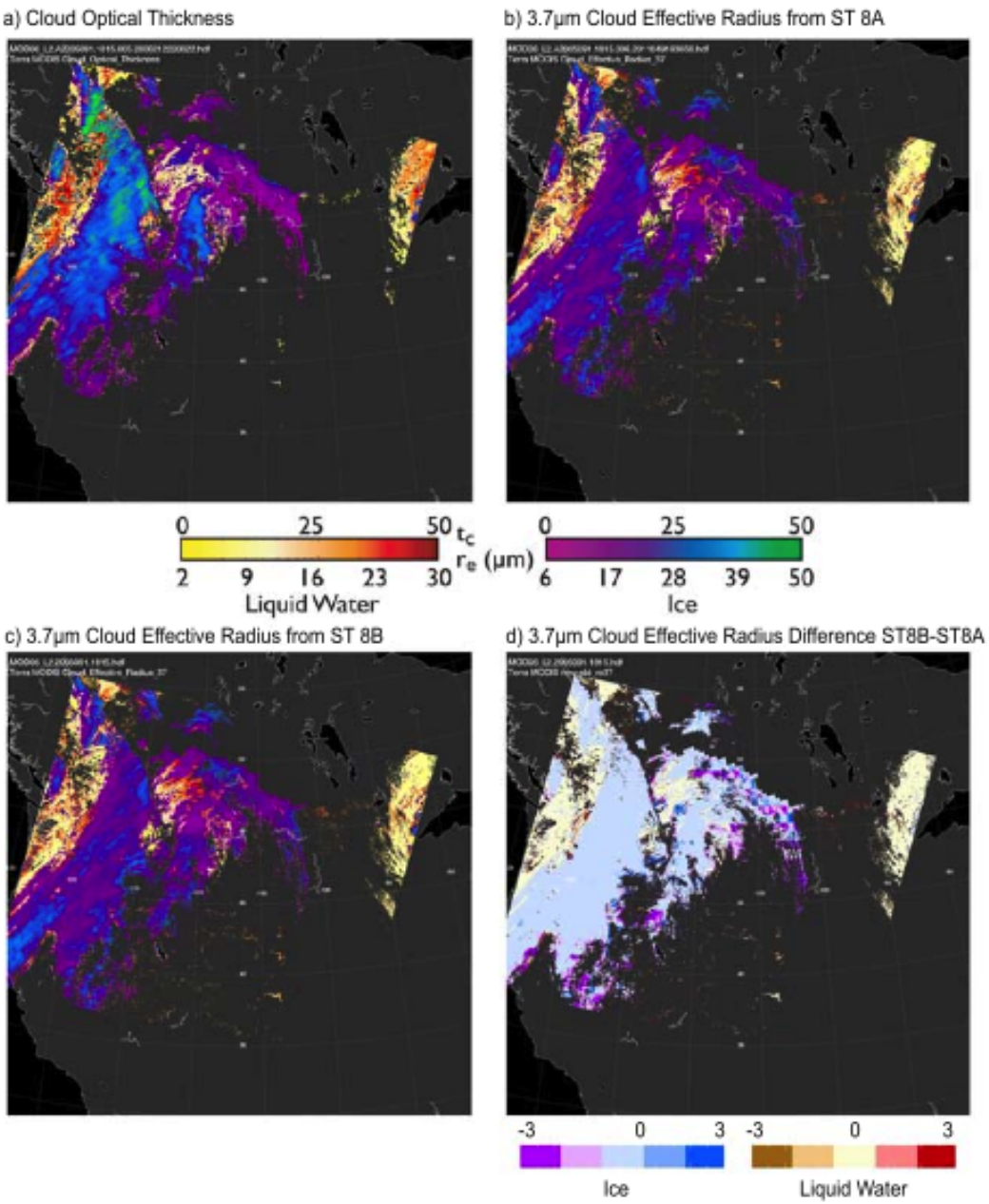

Figure 8: Terra MODIS 2005 day 091, 18:15 UTC, Western United States. The panels illustrate the impact of changes between science test 8A and 8B as cloud optical thickness in panel a), 3.7µm cloud effective radius from ST8A in panel b), 3.7µm cloud effective radius from ST8B in panel c) and the difference image in panel d)

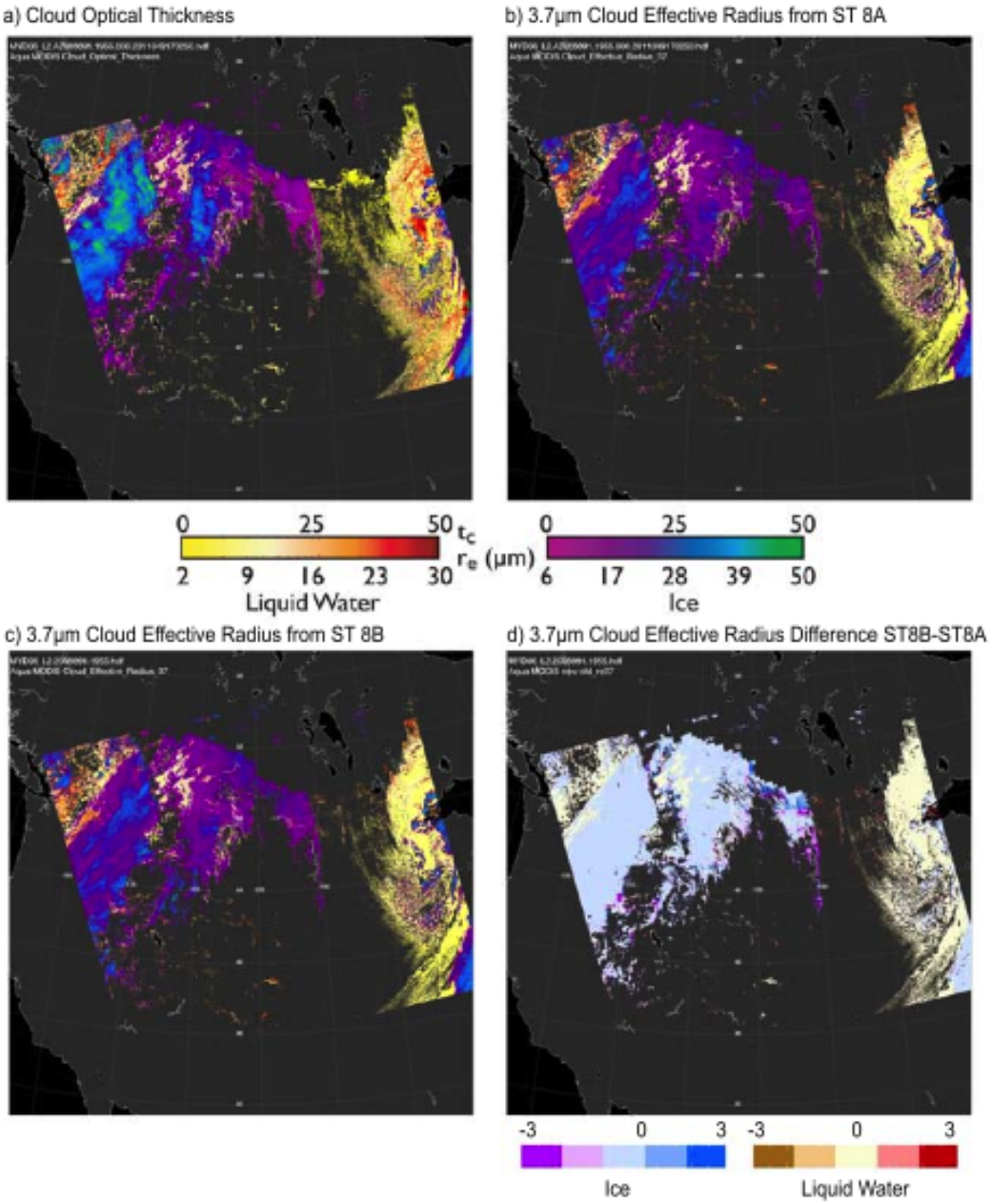

Figure 9: Aqua MODIS 2005 day 091, 19:55 UTC, Western United States. The panels illustrate the impact of changes between science test 8A and 8B as cloud optical thickness in panel a), 3.7µm cloud effective radius from ST8A in panel b), 3.7µm cloud effective radius from ST8B in panel c) and the difference image in panel d)

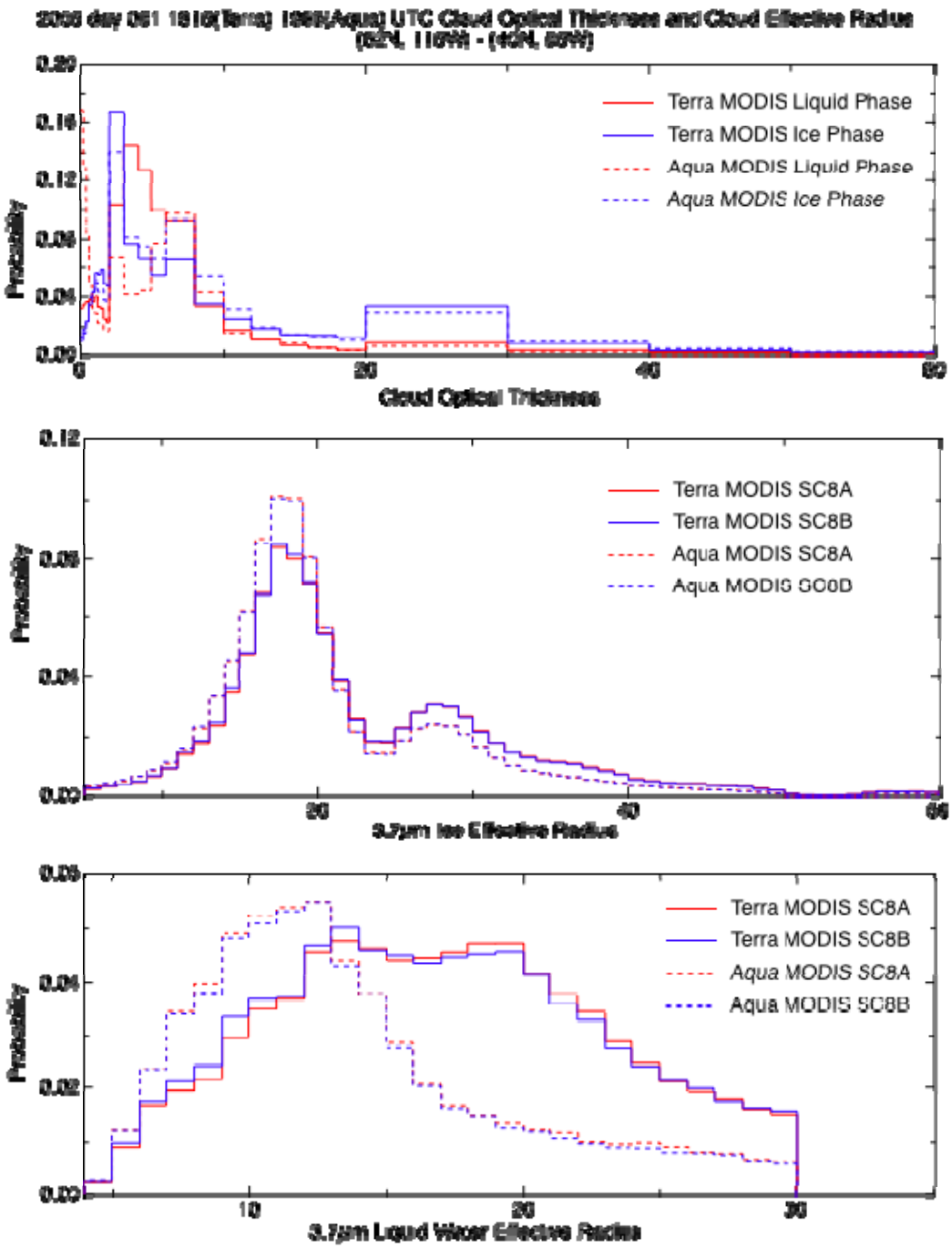

Figure 10: Histograms of retrieved optical thickness and 3.7μm cloud effective radius for the Western US case.

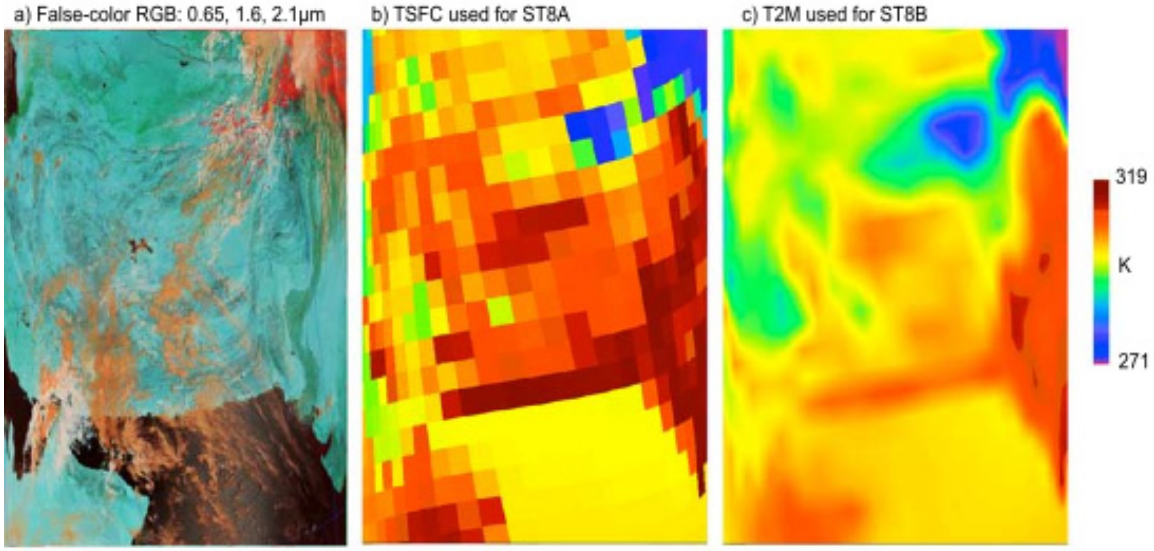

Figure 11: Terra MODIS 2005 day 109, 06:35 UTC. Panel a) shows the false-color RGB composite RGB: 0.65, 1.6, 2.1μm. Panel b) shows the original surface temperature field used in ST8A. Panel c) shows the new interpolated T2M-based surface temperature field.

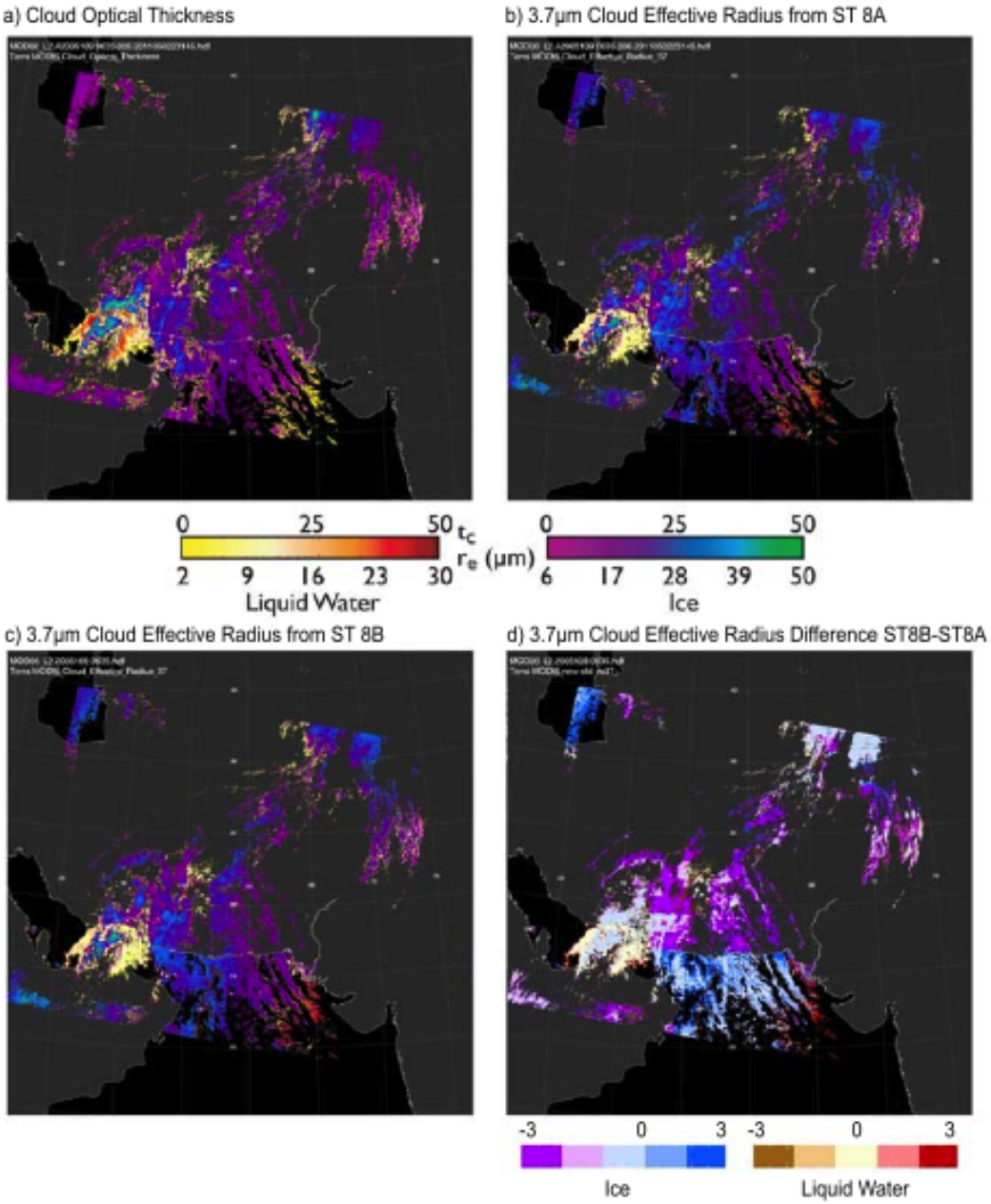

Figure 12: Terra MODIS 2005 day 109, 06:35 UTC, Northern Arabian Sea. The panels illustrate the impact of changes between science test 8A and 8B as cloud optical thickness in panel a), 3.7µm cloud effective radius from ST8A in panel b), 3.7µm cloud effective radius from ST8B in panel c) and the difference image in panel d)

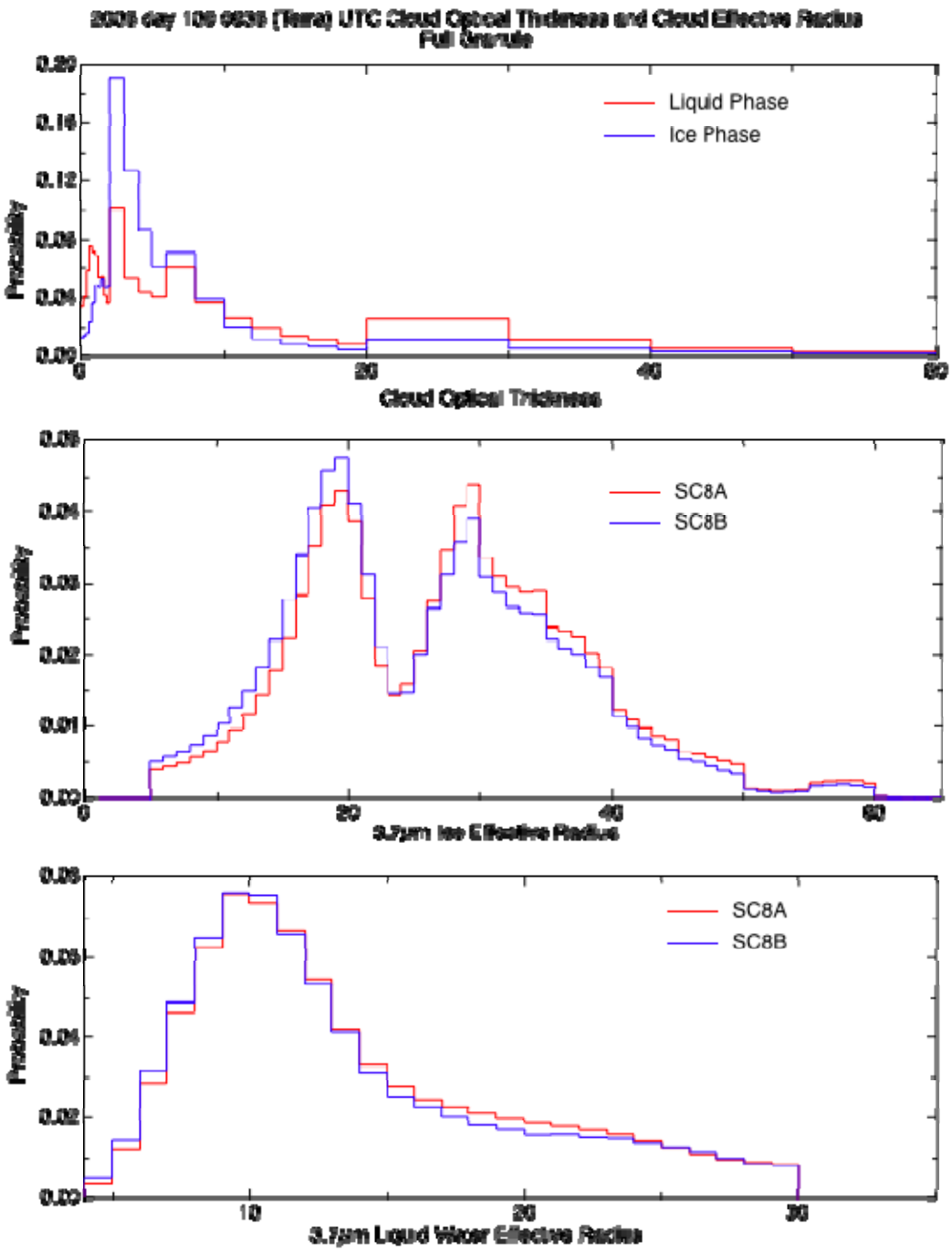

Figure 10: Histograms of retrieved optical thickness and 3.7μm cloud effective radius for the Arabian Sea I (Terra only) case.

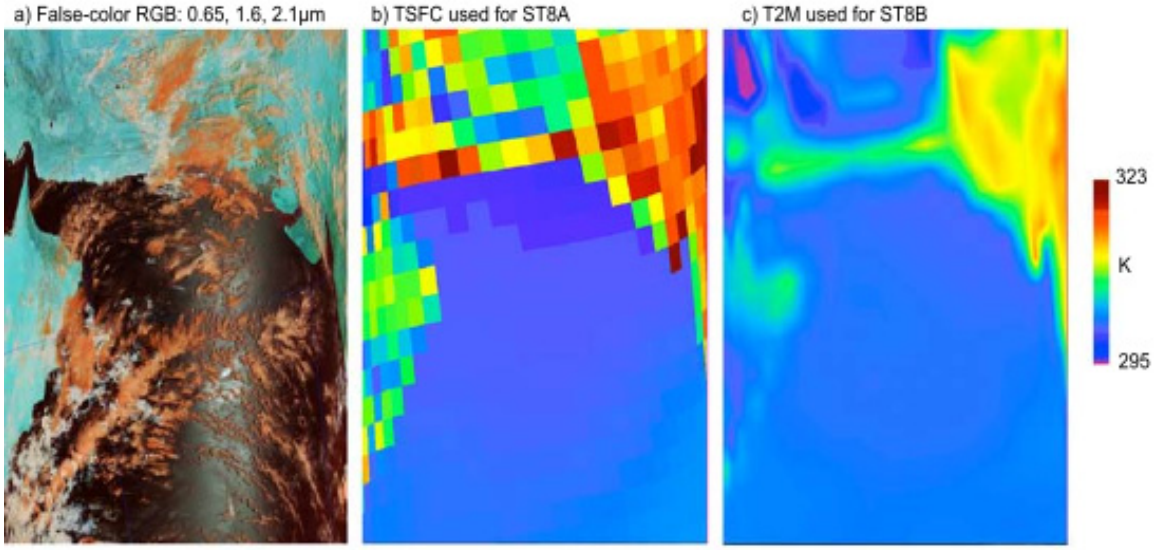

Figure 14: Terra MODIS 2005 day 111, 06:25 UTC. Panel a) shows the false-color RGB composite RGB: 0.65, 1.6, 2.1μm. Panel b) shows the original surface temperature field used in ST8A. Panel c) shows the new interpolated T2M-based surface temperature field.

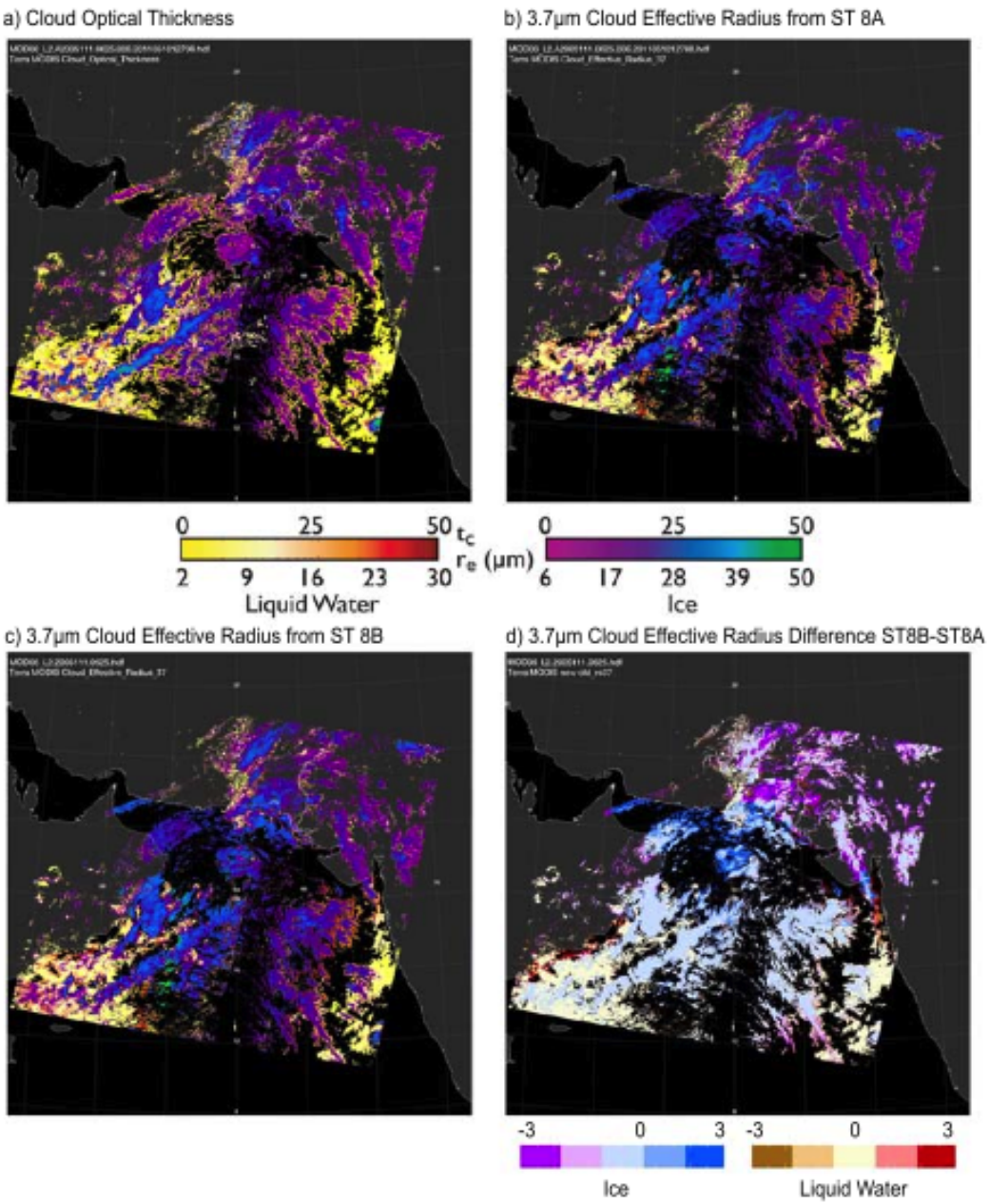

Figure 15: Terra MODIS 2005 day 111, 06:25 UTC, Arabian Sea. The panels illustrate the impact of changes between science test 8A and 8B as cloud optical thickness in panel a), 3.7µm cloud effective radius from ST8A in panel b), 3.7µm cloud effective radius from ST8B in panel c) and the difference image in panel d)

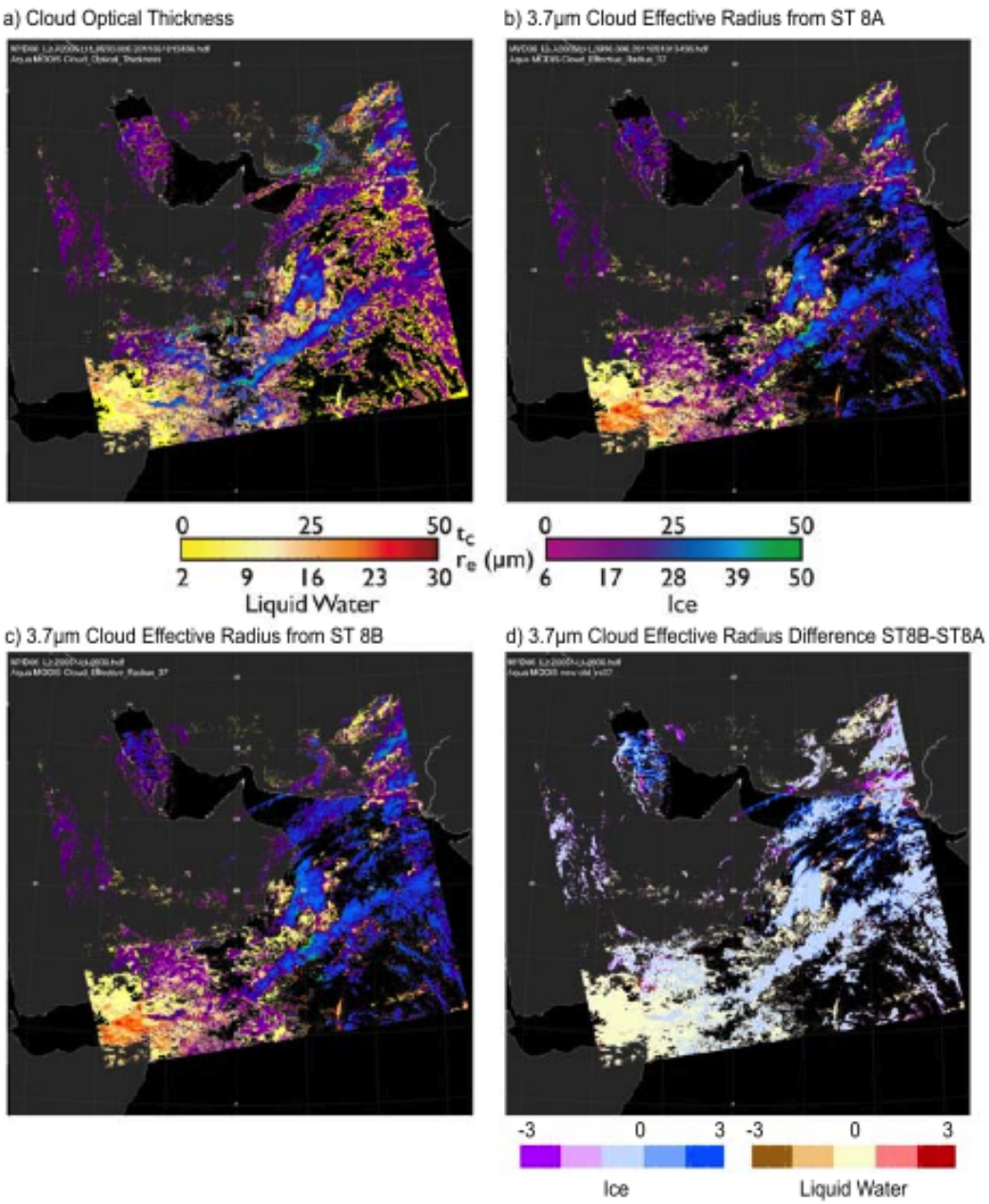

Figure 16: Aqua MODIS 2005 day 111, 09:30 UTC, Arabian Sea. The panels illustrate the impact of changes between science test 8A and 8B as cloud optical thickness in panel a), 3.7µm cloud effective radius from ST8A in panel b), 3.7µm cloud effective radius from ST8B in panel c) and the difference image in panel d)

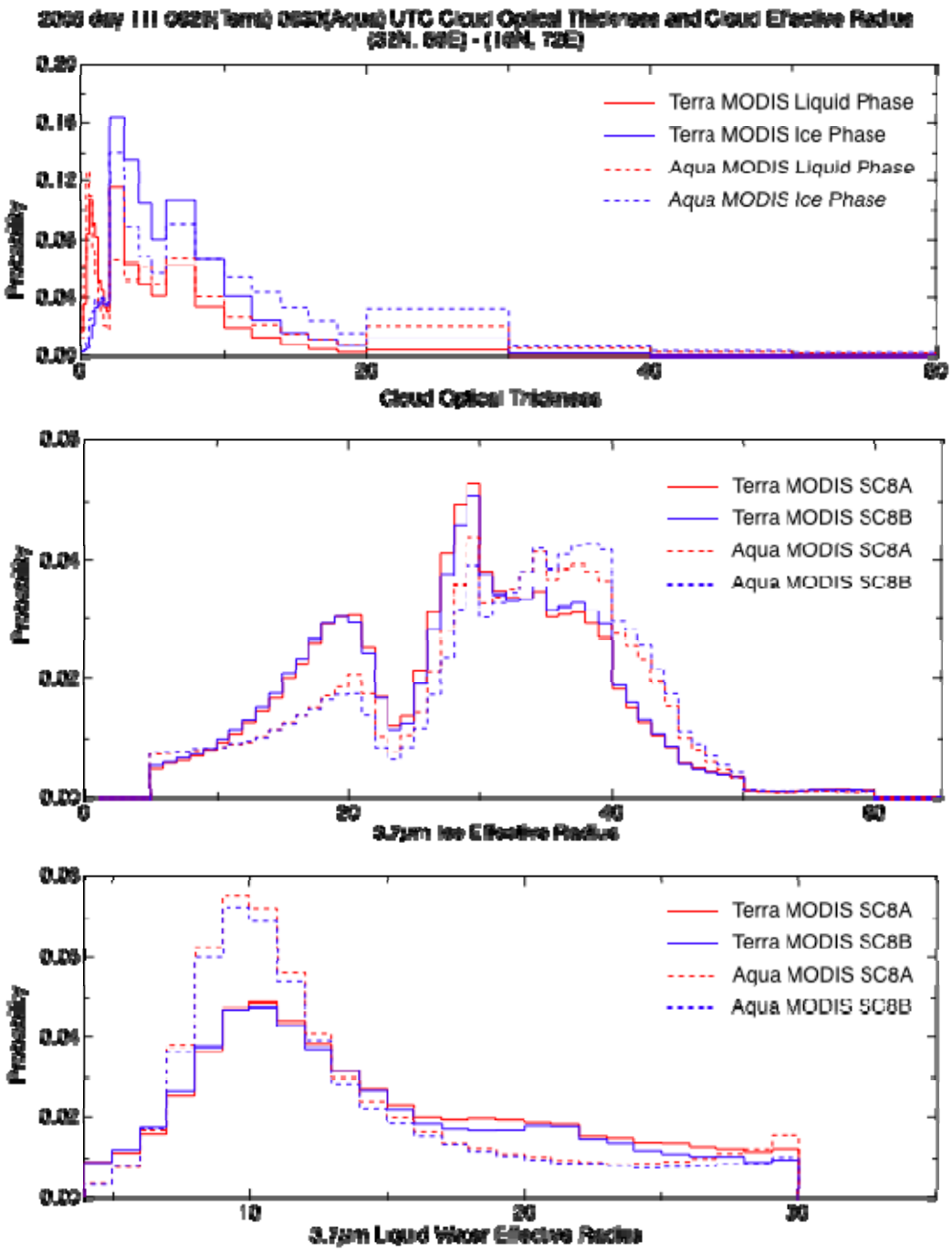

Figure 17: Histograms of retrieved optical thickness and 3.7μm cloud effective radius for the Arabian Sea II case.